JOURNAL OF MECHANICS OF CONTINUA AND MATHEMATICAL SCIENCES
www.journalimcms.org

ISSN (Online) : 2454 -7190 Vol.-21, No.-04, April (2026) pp 135-152 ISSN (Print) 0973-8975

EXPERIMENTAL INVESTIGATION OF A HYDROGEN-ENRICHED RCCI ENGINE FUELED WITH MICROALGAE BIODIESEL

Korukolu Ratna Raj[1], A. Saravanan[2]

[1]Department of Mechanical Engineering, Aditya University, Surampalem, India-533437.

[2]Department of Mechanical Engineering, Aditya University, Surampalem, India -533437.

Email: [1]ratnarajkorukolu@gmail.com, [2]saravanan.a@adityauniversity.in

Corresponding Author: **A. Saravanan**

https://doi.org/10.26782/jmcms.2026.04.00007

(Received: January 21, 2026; Revised: April 03, 2026; Accepted : April 17, 2026)

Abstract

The present study examines the impact of hydrogen induction on the performance and emission attributes of a Reactivity Controlled Compression Ignition (RCCI) Engine operating on a microalgae biodiesel–diesel blend (B20D80) with a constant injection timing of 23° BTDC and an injection pressure of 200 bar. Experiments were conducted with hydrogen induction at flow rates of 3, 6, and 9 lpm, referred to as B20D80 + H_2 3 lpm, B20D80 + H_2 6 lpm, and B20D80 + H_2 9 lpm, respectively. Among the tested fuel combinations, the B20D80 + H_2 9 lpm blend showed improved performance under these fixed injection conditions, achieving a 20.8% enhancement in brake thermal efficiency and a 28.1% decrease in brake specific fuel consumption compared to conventional diesel operation. Emission analysis indicated that hydrogen enrichment led to substantial reductions in major pollutants, carbon monoxide, and smoke opacity, decreasing by 24% and 25%, while carbon dioxide and hydrocarbon emissions were reduced by around 8.6% and 35%, owing to the carbon-free nature of hydrogen and the oxygenated structure of biodiesel. However, nitrogen oxide emissions increased moderately by 22.8%, which is due to higher in-cylinder temperatures resulting from enhanced combustion. Overall, the results demonstrate that hydrogen-assisted microalgae biodiesel operation significantly improves combustion efficiency while effectively reducing most exhaust emissions, highlighting its viability as a cleaner, more efficient dual-fuel strategy for RCCI engines.

Keywords: RCCI Engine, Performance, Hydrogen, Microalgae Biodiesel, Dual-Fuel

Nomenclature

RCCI	Reactivity Controlled Compression Ignition Engine
H_2	Hydrogen
BTDC	Before Top Dead Centre

BTE	Brake Thermal Efficiency
CO	Carbon Monoxide Emissions
HC	Hydrocarbon
CO_2	Carbon Dioxide
NO_x	Nitrogen Oxide
HRF	High Reactivity Fuel
LRF	Low Reactivity Fuel
ANN	Artificial Neural Network

I. Introduction:

The world's energy sector is rapidly changing, as global organizations promote zero-carbon emissions and encourage the adoption of renewable energy sources [VII]. Consequently, the dependence on fossil fuels is decreasing, whereas the demand for clean and sustainable energy is growing, reshaping the way energy is yielded and expended worldwide. The global energy sector is gradually shifting toward low-carbon and carbon-free energy, which means reducing carbon emissions from fuel and power production. This transition presents new challenges for IC engines, particularly decarbonization, which can be addressed by adopting sustainable alternative fuels and advanced combustion strategies that emit little or no carbon [XII]. To make combustion more efficient and cut down on emissions, new methods have been created, especially low-temperature techniques [XV], like HCCI, PCCI, and RCCI. Among them, RCCI engines have emerged as a promising solution because of the ability to use two fuels with different reactivities [I], providing better ignition control, enhanced combustion stability, and reduced pollutant formation. In RCCI engines, an LRF is typically introduced through the intake manifold [XVI], while an HRF is injected directly inside the combustion chamber. Compared to regular diesel engines, this dual fuel strategy makes the engine more fuel-efficient and produces fewer emissions. Optimal fuel injection time and pressure are critical, as these indicators influence ignition delay, combustion phasing, cylinder pressure, and overall engine performance. Early injection timing increases delay in combustion, causing high cylinder pressures, improved BTE, and reduced carbon monoxide and hydrocarbon emissions, though nitrogen oxide emissions may slightly increase. In contrast, late injection timing shortens the ignition delay, reduces cylinder pressure and BTE, raises the level of CO and HC emissions, and lowers nitrogen oxide [X].

Similarly, high injection pressure improves fuel atomization, increases fuel-air mixing, and enables more complete combustion [IX], whereas low injection pressure can lead to poor atomization, incomplete combustion, reduced BTE, and increased pollutant formation. By carefully balancing injection timing and pressure in RCCI engines, optimized combustion performance can be achieved while utilizing low-carbon renewable fuels [XIV]. In this way, RCCI engines not only address the internal challenges of IC engine decarbonization but also serve as an enabling technology that facilitates the adoption of sustainable fuels, supporting a comprehensive approach to reducing the carbon footprints of the transportation and energy sectors worldwide. Recently, many sustainable fuels such as alcohols, ethers, and esters have been studied as alternatives to fossil fuels. These fuels can reduce fossil fuel consumption, but they still release some carbon. Using zero-carbon alternatives, such as ammonia and hydrogen [III], is one of the most effective approaches to achieving zero-carbon emissions in IC engines. Halis et al. [V] have numerically studied the effect of injection timing on the RCCI engine and validated their findings using Converge CFD software. The findings revealed that injection timing significantly affects the RCCI engine, with higher injection timing leading to an increase in cylinder pressure and HRR. Yun-Young Ham et al. [IV] numerically analysed the impact of injection timing and the two stages of diesel fuel injection in an RCCI engine. The outcomes showed that advancing the first injection timing results in slower combustion, decreased combustion temperature, lower engine performance, and increased hydrocarbon and carbon monoxide emissions. The subsequent injection at 60˚ ATDC improved combustion and reduced emissions, while another injection set to 30˚ ATDC also yielded superior results.

Two-stage injection significantly reduced emissions and enhanced the performance of the RCCI engine compared to single injection timing. Motallibi Hasankola et al. [XIII] conducted an experimental investigation on the influence of injection timing on a diesel/gasoline RCCI engine with the injection timing ranging from 10˚ to 50˚ BTDC. The findings indicate that the greatest BTE and power were achieved at 40˚ BTDC, along with reduced PM but a slight increase in NOx emissions compared with other injection ranges. Rakesh et al. [XVIII] evaluated the performance and emission properties of hydrogen-diluted Waste Plastic Oil blended with diesel in a PCCI engine through different injection timings. The results showed that 23˚ bTDC was the best timing with improved BTE and better emission control than diesel. Althmakuri Ashok et al. [II] have studied the impact of injection timing on the RCCI engine by using a Jatropha oil-diesel blend with 1-pentanol. The injection angles vary between 19˚, 21˚, 23˚, 25˚, and 27˚ before top dead centre. With a fixed injection pressure of 600 bar, the study indicated that improving the angle of injection leads to improved performance of the engine with reduced pollutants. The 25˚ BTDC provides the greatest BTE and decreased carbon monoxide and hydrocarbon emissions with increased NOx in comparison to the remaining injection angles.

Jatadhara et al. [VI] conducted an experimental analysis to explore the impact of injection timing in the dual fuel engine by mixing diesel with Karjana Oil methyl esters, plastic pyrolysis, and ethanol as LRFs, using the injection timings of 40˚, 45˚, and 50˚ATDC. Among these, the injection time at 45˚ ATDC produces the maximum BTE and reduces carbon monoxide and hydrocarbon emissions compared with other timings, but NOx increased for all three injection timings. V.S. Kumbhar et al. [VIII] explored how injection pressure affects the RCCI engine by using blends of ethanol, gasoline, diesel, and biodiesel, with the injection pressure between 400 bar and 700 bar and loads between 0 and 12 kg. The results show that the higher injection pressure leads to increased charge homogeneity, reduced combustion duration, and increased energy release rate. At 700 bar, the thermal efficiency was improved, and soot, HC, and CO emissions were decreased, while NOx was increased. P.V Elumalai [XIX] analysed the impact of graphene oxide nanoadditives on Tamanu Methyl Ester biodiesel in a CI engine under various running conditions. It was found that the use of TME20+G050 blend provided better efficiency and reduced emissions, showing its capability as an efficient fuel option.

II. Motivation and Objective of this Research:

The limitations of fossil fuels and growing demand for sustainable energy have made microalgae biodiesel a highly promising alternative fuel for IC engines due to its renewable nature, high productivity, and potential to reduce emissions. However, the performance and emission behaviour of engines operating with biodiesel are strongly dependent on injection strategies. In RCCI engines, injection timing and injection pressures are the most important parameters for controlling combustion phasing, fuel atomization, and emission formation. Improper injection timing may lead to increased combustion delay and higher nitrogen oxide formation; meanwhile, improper pressure can result in insufficient atomization and reduced thermal efficiency. Therefore, optimizing these parameters is essential to achieve improved combustion efficiency and lower emissions. In this context, the current study evaluates the performance and emission behaviour of an RCCI engine operated at a fixed injection timing of 23° BTDC and an injection pressure of 200 bar using microalgae biodiesel as HRF and hydrogen supplied at flow rates of 3, 6, and 9 lpm as LRF. This study focuses on analysing the impact of hydrogen enrichment under constant injection conditions. Furthermore, an ANN model is employed to predict the engine performance and emissions characteristics based on experimental data.

III. Materials and Methods:

Biodiesel Production from Microalgae:

Microalgae are third-generation feedstocks that can grow in seawater and soil ecosystems. It looks like a normal plant; it possesses higher lipid content and greater photosynthetic efficiency compared with other plants due to its unique cellular structure and adaptive metabolism. Therefore, microalgae are considered one of the most promising renewable sources for biodiesel production [XI]. The process of converting microalgae culture into the required biomass is illustrated in Fig 1.

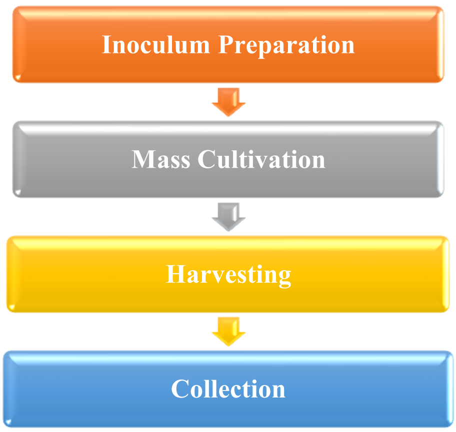

Fig.1 Illustrates the process of converting microalgae into biomass.

Extraction and Transesterification Process of Microalgae:

It is a technique used to separate the lipids from cultivated microalgae cells to produce beneficial products such as biodiesel, dietary supplements, and pharmaceuticals. After cultivation of microalgae, which will store their oil content in their tiny cells to form the triacylglycerol. Special strategies are utilized to collapse the cell walls in the stored medium and extract the oil from the microalgae cells. It can be implemented in different forms, like mechanical extraction (expelling or grinding), extraction by solvents (using chemicals like hexane or methanol), and enzyme extraction (enzymes). The extracted microalgae lipids were transformed into biodiesel through the process of transesterification using a base catalyst. The lipid was preheated to approximately 55˚C to reduce its viscosity. The methoxide solution was made by adding 1 wt.% of KOH into the methanol, maintaining a methanol-to-oil ratio of 6:1. The methoxide solution was slowly mixed with warm oil, and the solution was agitated for one hour while maintaining a temperature between 55 and 60˚C. This mixture was permitted to settle in a separating funnel for 10-12 hours, resulting in the formation of two layers. The top layer consisted of biodiesel, and the bottom layer contained glycerol [XVII]. The biodiesel layer was carefully collected and washed with warm distilled water to remove traces of catalyst and methanol, and then dried at 110˚C to remove moisture. Finally, the refined biodiesel was filtered and stored in airtight bottles until further use.

Hydrogen:

Hydrogen is a carbon-free energy carrier that has attracted increasing attention as an auxiliary fuel for advanced IC engines. It is suitable for RCCI operation due to its high-octane number, wide flammability limits, and rapid diffusivity. These properties allow for stable lean combustion and enhanced thermal efficiency. Hydrogen does not exist in a free state in nature and therefore must be produced. It can be generated through several methods, such as steam methane reforming, electrolysis of water, biomass or coal gasification, and industrial by-product recovery. The properties of diesel, biodiesel, and hydrogen are presented in the Table.1

Table 1: Physicochemical Characteristics of diesel and Microalgae biodiesel.

S. No.	Diesel	Microalgae biodiesel	Hydrogen
Density (kg/m^3)	844	880-900	682
Viscosity	2-4 mm^2/s	4-6 mm^2/s	0.0084 CP
Calorific value (MJ/kg)	41.82	36-40	120-142
Cetane/octane number	45-55	45-55	Octane-130
Flash point (˚C)	52-96	120-180	-253
Autoignition temp (˚C)	210	200-220	585
Carbon content (%)	86	77	0

Experimental Procedure:

The experimental study was conducted on an RCCI engine operating through a dual-fuel strategy. The specifications of the test engine used in this research are provided in Table 2. Fig. 2 illustrates the experimental setup, where hydrogen was supplied as LRF through the intake manifold, while the microalgae-biodiesel-diesel blend served as a high-reactivity fuel. A high-pressure composite cylinder was used to store the hydrogen and delivered through dual-stage pressure regulators to maintain a stable delivery pressure suitable for port fuel injection, which allowed sufficient premixing of the hydrogen with the intake air. During the experiments, hydrogen was supplied at controlled flow rates of 3 lpm, 6 lpm, and 9 lpm to evaluate the influence of hydrogen energy share on dual fuel operation. The hydrogen flow rates were controlled to vary the energy share at a constant engine condition. The hydrogen volumetric flow rates were transformed into mass flow rates by utilizing the density of hydrogen (0.0899 kg/m^3). The resulting mass flow rates for three different flow rates were 4.49×10^{-6} kg/s, 8.99×10^{-6} kg/s, and 1.34×10^{-5} kg/s, respectively. The energy input due to hydrogen was determined using its lower heating value of hydrogen, which is 120 MJ/kg. The energy share due to hydrogen is given by the following equation: 1

$$\text{Energy Share}_{H_2} = \frac{\dot{m}_{H_2} \times LHV_{H_2}}{\dot{m}_{B20D80} \times LHV_{B20D80} + \dot{m}_{H_2} \times LHV_{H_2}} \times 100 \qquad (1)$$

The hydrogen contributes 5-20% of the total fuel energy input. Initially, the B20D80 blend was prepared by mixing 20% microalgae biodiesel with 80% conventional diesel. The fuel was delivered through a high-pressure common-rail system with a maximum pressure of 200 bar and injected directly into the combustion chamber at a 23° crank angle before top dead centre using a single-hole nozzle, which helped create a regulated charge and monitor heat release.

Fig. 2: Experimental Setup

The timing and quantity of each fuel were controlled independently using separate control units, allowing precise adjustment of the reactivity gradient within the cylinder. This coordinated technique effectively harnessed the rapid ignition behaviour of hydrogen to initiate combustion, while utilizing the oxygen-rich, slower-burning characteristics of algae biodiesel to sustain heat release throughout the expansion stroke. This also ensures proper blending of hydrogen with the intake air entering the combustion chamber. The detailed fuel test matrix is listed in Table 3. The B20D80 blend was injected directly as high-reactivity fuel through the diesel injector to initiate the controlled ignition. The engine was run at steady state operating parameters, and for every fuel mixture, the cylinder pressure, combustion phasing, emissions, and performance data were continuously recorded.

Table 2: Specifications of test engine

Parameters	Details
Engine Make	Kirloskar
Engine Power	5.20 kW
Speed of the Engine	1500 rpm
No of Cylinders	1
Number of Strokes	4
Cooling Type	Water
Bore and stroke	87.50 mm and 110 mm
Length of connecting rod	234 mm
Dynamometer	Eddy Current

Table 3: Fuel Test Matrix

Sample No.	Fuel Composition
1	Diesel
2	B20D80 + H_2 3 LPM
3	B20D80 + H_2 6 LPM
4	B20D80 + H_2 9 LPM

IV. Results and Discussions:

Performance Analysis:

Brake Thermal Efficiency:

Brake thermal efficiency (BTE) indicates the ability of an engine to transform the chemical energy of fuel into mechanical output. From Fig. 3, the B20D80 + H_2 9 LPM blend had the highest BTE under the tested conditions, showing an improvement of 20.81% compared with diesel. This value has been improved by the synergistic action of microalgae biodiesel and hydrogen in RCCI combustion. The high cetane number and oxygenated nature of microalgae biodiesel facilitate better ignition quality and more stable combustion, which will ensure minimal combustion delay and reduced incomplete burning losses. Meanwhile, hydrogen enrichment increases the rate of combustion owing to high flame speed, extensive flammability, and rapid diffusivity, and also contributes additional energy input, which results in a quicker and smoother heat release nearer the top dead centre, where energy conversion is more efficient. In addition to that, hydrogen allows for lean burning that minimizes heat losses and enhances thermal efficiency. The B20D80 + H_2 6 lpm and B20D80 + H_2 3 lpm blends also showed improvements in BTE of 15.64% and 7.84%, respectively. Overall, the findings affirm that hydrogen-assisted microalgae biodiesel combustion is very effective in improving the BTE at all load conditions, compared to normal diesel operation.

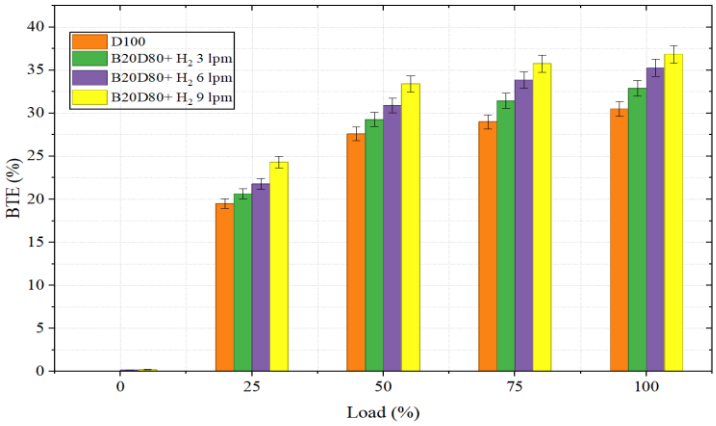

Fig.3. BTE Vs. Load for all tested blends.

Brake Specific Fuel Consumption:

From Fig 4, the highest reduction of BSFC was recorded for the B20D80 + H_2 9 lpm blend, which recorded a reduction of 28.1% compared to conventional diesel, showing improved fuel utilization under the present experimental conditions. The noteworthy decrease is mainly due to hydrogen's elevated flame speed, wide flammability, and increased oxidation of fuel, and the oxygen-rich nature of microalgae biodiesel facilitates more complete combustion, producing minimal unburned fuel. The next lowest BSFC was observed for the B20D80 + H_2 6 lpm blend, which showed a 25% decrease due to moderate hydrogen enrichment improving mixture reactivity and fuel utilization efficiency. A reduction of 18.8% in BSFC was observed for the B20D80 + H_2 3 lpm blend, proving that even low-rate hydrogen supplementation can effectively improve fuel economy. In comparison, the conventional diesel operation resulted in the highest BSFC because of relatively slower fuel oxidation and higher fuel consumption for the same engine power output.

In dual fuel mode, the total energy input consists of B20D80 and hydrogen. Thus, the decrease in BSFC will be affected not only due to better combustion efficiency but also due to an increase in energy input from hydrogen. Thus, BSFC is normalized based on the total fuel energy input, including the contribution from hydrogen, ensuring consistency across all fuel cases.

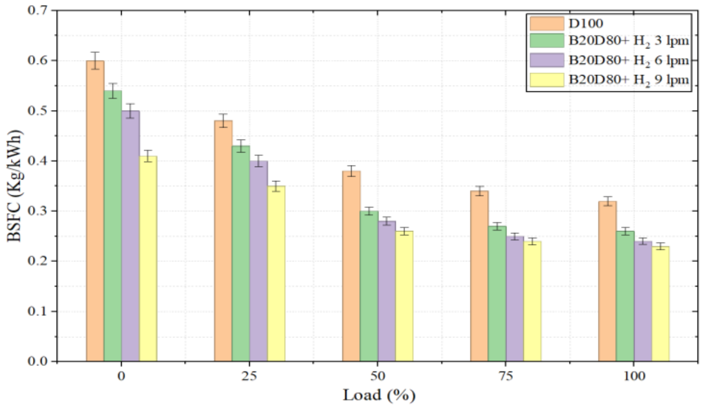

Fig.4. BSFC Vs. Load for all tested blends.

Emissions:

Carbon Monoxide:

It is the key parameter of combustion quality in IC engines. Elevated carbon monoxide levels generally signify incomplete combustion due to insufficient oxygen or poor air mixing. Carbon monoxide (CO) emissions tend to increase with engine load for all fuel combinations, as richer mixtures are formed at higher loads, reducing the availability of oxygen required for complete combustion, as shown in Fig 5.

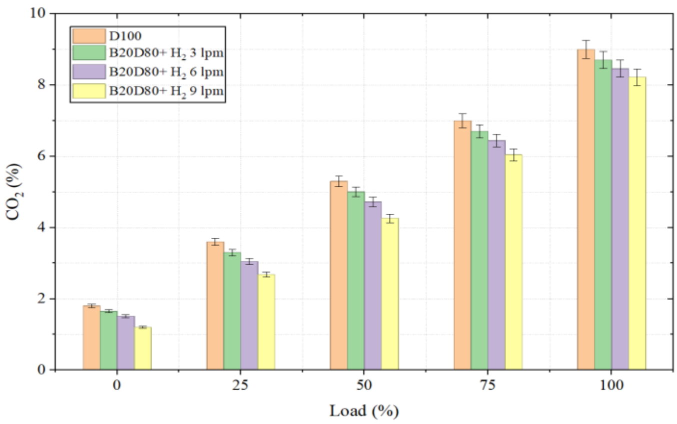

Fig.5. CO Vs. Load for all tested blends.

At full load, the blend B20D80 + H_2 9 lpm exhibits the maximum reduction in CO emissions under tested conditions, with a value of 0.070%, corresponding to a reduction of about 24% compared to neat diesel (0.092%). This is followed by B20D80 + H_2 6 lpm, which shows CO emission of around 0.087%, representing a reduction of 5.4% compared to diesel. Similarly, B20D80 + H_2 3 lpm results in CO emissions of 0.089%, indicating a reduction of 3.2% relative to diesel operation. The progressive decrease in CO emissions with rising hydrogen flow rate is primarily attributed to improved flame propagation, enhanced combustion completeness, and more oxidation of CO into CO_2 due to hydrogen enrichment.

Hydrocarbons:

Hydrocarbon emissions arise from unburnt or partially burnt fuel, which occurs due to poor air mixing, wall quenching, and incomplete combustion. A decreasing trend in hydrocarbon emissions is observed with hydrogen enrichment across the entire range of engine loads, owing to improved combustion characteristics, as illustrated in Fig 6. Among the tested fuel combinations, B20D80 + H_2 9 lpm shows the highest reduction in HC emissions, with a value of 82 ppm, corresponding to a maximum reduction of about 25% compared to neat diesel (110 ppm), particularly at low and high load conditions. This reduction is attributed to faster flame propagation and improved mixture reactivity. The next significant reduction is observed for B20D80 + H_2 6 lpm, which shows HC emissions (83 ppm), representing a reduction of about 24% compared to diesel. This improvement is mainly due to reduced ignition delay time and increased premixed combustion phase. On the other hand, B20D80 + H_2 3 lpm exhibits the HC emissions (97 ppm), corresponding to a reduction of 11.82%, which is relatively lower due to limited hydrogen availability and weaker enhancement in chemical reactivity. Overall, hydrogen-assisted B20D80 blends significantly suppress HC emissions formation across all engine loads due to cleaner and more complete combustion under RCCI engine operation.

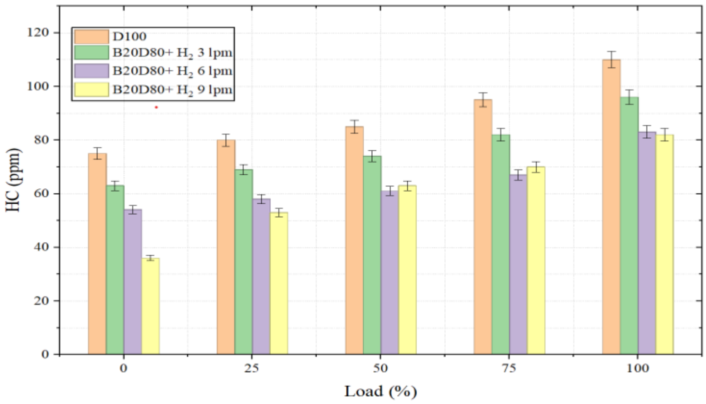

Fig.6. HC Vs. Load for all tested blends.

Carbon Dioxide:

Carbon dioxide is directly caused by the carbon content in the fuel and the nature of the combustion behaviours inside the engine. As illustrated in Fig 7, carbon dioxide emissions show a gradual decrease for biodiesel-hydrogen blends across all engine loads. This reduction is mainly attributed to hydrogen enrichment, which partially replaces carbon-based diesel with biodiesel fuel. At full load, B20D80 + H_2 9 lpm shows the highest reduction in CO_2 emissions, with a decrease of 8.7% compared to diesel. This is followed by B20D80 + H_2 6 lpm, B20D80 + H_2 3 lpm, which show reductions of 6% and 3.3%, respectively. The observed trend is primarily due to the carbon-free nature of hydrogen, along with its high flame speed and wide flammability limits, which enhance combustion efficiency and mixture uniformity. These factors reduce carbon-based oxidation products while maintaining efficient combustion across all engine loads.

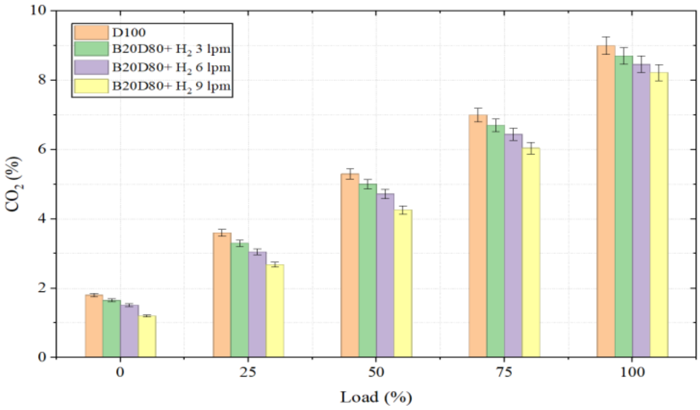

Fig.7. CO_2 Vs. Load for all tested blends.

Nitrogen Oxide:

NO_x emissions are primarily formed due to elevated cylinder temperatures and the reaction between nitrogen and oxygen during combustion. They serve as an important indicator of combustion and temperature, and efficiency within the engine. NOx emissions increase with engine load for all fuel combinations due to high cylinder temperatures and increased HRR, as presented in Fig 8. Among the investigated fuels, neat diesel consistently exhibits the lowest NOx emissions, whereas hydrogen-enriched B20D80 blends show higher NOx formation, which increases with rising hydrogen flow rates. At full load, NOx emissions increase from 1900 ppm (diesel) to 2080 ppm for B20D80 + H_2 3 lpm, representing an increase of 9.5%. Further increases are observed for B20D80 + H_2 6 lpm (2251 ppm) and B20D80 + H_2 9 lpm (2334 ppm), representing an increase of 18.5% and 22.8%, respectively. The highest NOx emissions are recorded for B20D80 + H_2 9 lpm.

This increase is attributed mainly to the fast-burning nature of hydrogen and the subsequent rise in the in-cylinder temperature levels, along with advanced combustion phasing. A fast combustion process reduces the ignition delay period; the prolonged period of high temperatures leads to increased NOx formation via the Zeldovich mechanism. Hence, the thermodynamic relationship between the energy liberation, temperature behaviour, and duration of the combustion process controls NOx emissions.

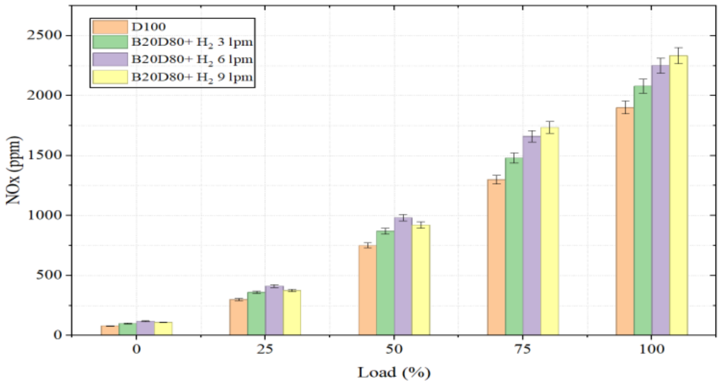

Fig.8. NOx Vs. Load for all tested blends

Smoke Opacity:

Smoke opacity is an important indicator of particulate matter concentration in engine exhaust and is usually associated with incomplete combustion in diesel engines. The variation of smoke opacity with engine load for the tested blends is shown in Fig 9. A significant reduction in smoke is observed with hydrogen-enriched blends across all load conditions. At full load, B20D80 + H_2 9 lpm exhibits the maximum reduction in smoke, with a decrease of 25% compared to diesel. This is followed by B20D80 + H_2 6 lpm and B20D80 + H_2 3 lpm, which show reductions of 11% and 6%, respectively. The reduction in smoke becomes more pronounced at higher loads due to increased fuel input, where hydrogen's rapid and clean combustion suppresses smoke formation effectively. This trend is primarily attributed to the carbon-free nature of hydrogen, its high flame speed, and improved combustion characteristics. Additionally, the inherent oxygen content in biodiesel enhances oxidation of soot precursors, thereby reducing particulate formation and overall smoke emissions.

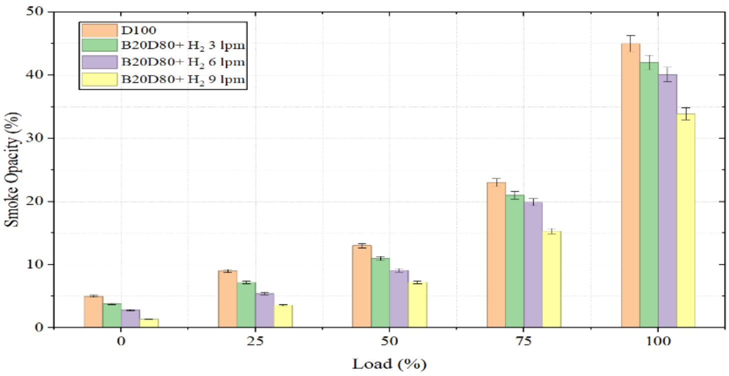

Fig.9. Smoke Vs. Load for all tested blends.

Combustion Characteristics

Cylinder Pressure :

Fig.10 demonstrates the variation of cylinder pressure for various fuel blends. The maximum in-cylinder pressure of 73.4 bar was recorded for B20D80+H_2 9 lpm, showing an increase of approximately 4.2% compared to diesel. This enhancement is mainly attributed to the combined effects of oxygen-rich microalgae biodiesel and hydrogen enrichment. The presence of hydrogen, with its high flame speed and rapid combustion characteristics, promotes faster heat release and improved combustion efficiency, resulting in a higher peak in-cylinder pressure.

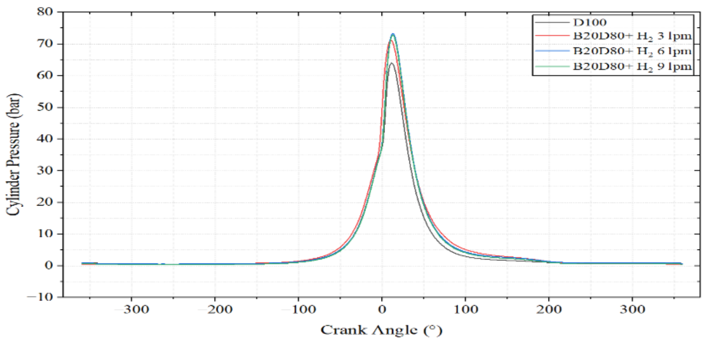

Fig.10. Crank Angle Vs. Cylinder Pressure for all blends

Heat Release Rate:

HRR shows the rate at which energy is released in the form of heat during the combustion process, and it is estimated using first law analysis based on in-cylinder pressure data. The highest HRR was achieved at B20D80+ H_2 9 lpm, as shown in Fig 11, indicating an improvement of 7% compared to the diesel. This improvement is attributed to the combined effects of biodiesel and hydrogen. In contrast, B20D80+ H_2 3 lpm and B20D80+ H_2 6 lpm exhibit smaller improvements in HRR due to lower hydrogen flow, which limits the extent of flame propagation enhancement and premixed combustion.

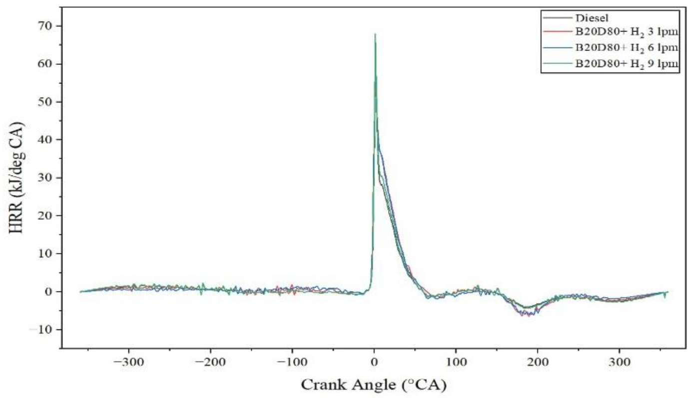

Fig. 11. Crank Angle Vs. Heat Release Rate for all blends.

The global equivalence ratio was analysed by considering the combined mass flow rate of diesel fuel and hydrogen gas. With increasing hydrogen flow from 3 to 9 lpm, the fuel-air mixture becomes leaner owing to its high diffusivity and gaseous state, enabling better mixing with the intake air. During RCCI combustion, the formation of reactivity stratification is achieved by blending hydrogen with B20D80 fuel.

Stratification is not significant at lower hydrogen flow levels due to insufficient hydrogen quantity. Moderate hydrogen flow improves the mixing of fuel with air, forming a larger reactivity gradient. High hydrogen flow strengthens stratification, producing an even mixture and faster combustion with better heat release characteristics. The findings show that the incorporation of hydrogen causes leaner combustion, which improves the mixing process and enhances the combustion process. In addition, combustion timing metrics such as CA10, CA50, and CA90 were established by analysing the cumulative heat release. The results indicate that the CA50 moves towards the top dead centre position with hydrogen addition, signifying an advanced combustion process, while decreased combustion duration suggests faster combustion.

V. ANN Report:

An artificial neural network model was developed to predict and validate the nonlinear behaviour of engine performance and emission attributes under various experimental conditions. The network was built in a mathematical computing environment, with engine load and fuel blend ratio as input parameters. The ANN was designed to predict key output responses, including brake thermal efficiency, brake specific fuel consumption, hydrocarbons, carbon monoxide, carbon dioxide, nitrogen oxides, and smoke. For strong generalization, the experimental dataset was randomly divided and distributed into 70% training data and 30% testing and validation data. The trained ANN showed a high degree of similarity between predicted and experimental values, proving its effectiveness in capturing the nonlinear relationships between operating parameters and engine performance and emission characteristics. The optimal ANN configuration was determined using a trial-and-error approach, where various network architectures were evaluated by varying the number of hidden neurons and training parameters. Fig 12 represents the surface plots for engine performance and emission characteristics. For each configuration, the network performance was evaluated using statistical indicators such as the coefficient of regression (R) and mean squared error (MSE). The architecture yielding the maximum R value and the minimum MSE values was selected as the optimal model. The obtained R-values for BTE, BSFC, HC, CO, CO_2, soot, and NOx are 0.9537, 0.9889, 0.960, 0.9507, 0.9696, 0.8410, 0.9860, and the mean square errors are 0.0468, 0.0091, 0.0144, 0.0387, 0.0335, 0.1423, 0.0136.

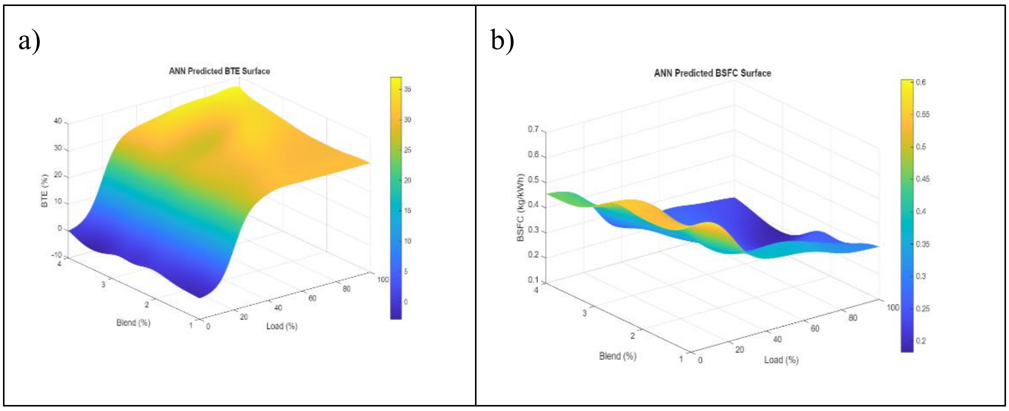

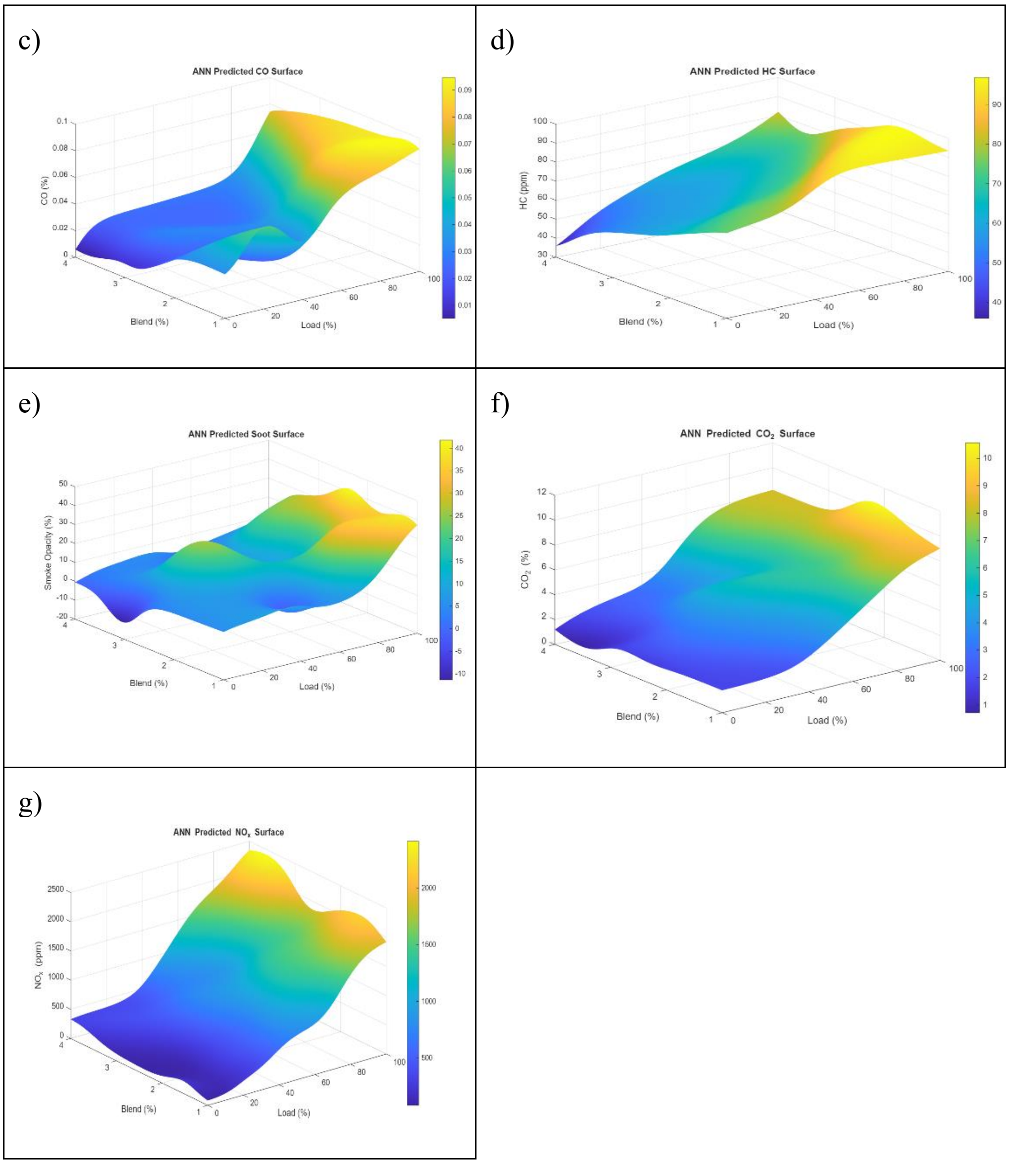

Fig. 12. Surface Plots for Engine Performance& Emissions

VI. Conclusions:

The B20D80 + H_2 (9 lpm) blend showed the highest improvement, achieving a 20.81% increase in BTE at full load compared to diesel under fixed injection conditions. Additionally, this blend B20D80+ H_2 9 lpm indicated the lowest BSFC, with a 28.1% at full load. Significant emission reductions were also observed in CO, HC, and smoke emissions, decreasing by 24%, 25%, and 25%, respectively, while CO_2 was reduced by 8.7%. However, NOx emissions increased by 22.8% at full load due to higher combustion temperatures inside the cylinder, under the selected operating conditions. Furthermore, the combustion behaviour of the B20D80 + H_2 9 lpm recorded the greatest improvements, with in-cylinder pressure enhanced by 4.2%, and the heat release rate was improved by 7% compared to diesel operation.

The integration of microalgae biodiesel with hydrogen significantly enhances the engine performance, while substantially reducing the emissions. The results highlight the strong potential of hydrogen-enriched biodiesel blends as cleaner and more sustainable alternative fuels for engine applications.

Conflict of Interest

There was no relevant conflict of interest regarding this paper.

References:

I. Armin, M., & Gholinia, M. (2022). Comparative evaluation of energy, performance, and emission characteristics in dual-fuel (CH4/Diesel) heavy-duty engine with RCCI combustion mode. *Results in Engineering*, *16*, 100766. 10.1016/j.rineng.2022.100766

II. Ashok, A., Gugulothu, S. K., Reddy, R. V., & Burra, B. (2022). Influence of fuel injection timing and trade-off study on the RCCI engine characteristics of Jatropha oil-diesel blend under 1-pentanol dual-fuel strategies. *Environmental Science and Pollution Research*, *30*(44), 98848–98857. 10.1007/s11356-022-22039-3

III. Dinesh, M. H., Pandey, J. K., & Kumar, G. N. (2022). Study of performance, combustion, and NOx emission behavior of an SI engine fuelled with ammonia/hydrogen blends at various compression ratio. *International Journal of Hydrogen Energy*, *47*(60), 25391–25403. 10.1016/j.ijhydene.2022.05.287

IV. Fakhari, A. H., Shafaghat, R., & Jahanian, O. (2020). Numerical Simulation of a Naturally Aspirated Natural Gas/Diesel RCCI Engine for Investigating the Effects of Injection Timing on the Combustion and Emissions. *Journal of Energy Resources Technology*, *142*(7), 072301. 10.1115/1.4046470

V. HaliS, S., Solmaz, H., Polat, S., & Yücesu, H. S. (2022). Numerical Study of the Effects of Lambda and Injection Timing on RCCI Combustion Mode. *International Journal of Automotive Science and Technology*, *6*(2), 120–126. 10.30939/ijastech..1105470

VI. Jatadhara, G. S., Chandrashekhar, T. K., Banapurmath, N. R., & Harari, P. A. (2023). Experimental investigation on the effect of injection timing and injection duration of low reactive fuels on RCCI mode of combustion operated with plastic pyrolysis oil. *Materials Today: Proceedings*, S2214785323046655. 10.1016/j.matpr.2023.09.006

VII. Kocak, E., & Alnour, M. (2022). Energy R&D expenditure, bioethanol consumption, and greenhouse gas emissions in the United States: Non-linear analysis and political implications. *Journal of Cleaner Production*, *374*, 133887. 10.1016/j.jclepro.2022.133887

VIII. Kumbhar, V. S., Shahare, A. S., & Awari, G. K. (2021). Influence of injection pressure on performance and emission characteristics of single cylinder RCCI engine fuelled with ethanol gasoline and diesel biodiesel blends. *Journal of Physics: Conference Series*, *2070*(1), 012160. 10.1088/1742-6596/2070/1/012160

IX. Li, J., Yang, W. M., Goh, T. N., An, H., & Maghbouli, A. (2014). Study on RCCI (reactivity controlled compression ignition) engine by means of statistical experimental design. *Energy*, *78*, 777–787. 10.1016/j.energy.2014.10.071

X. Madihi, R., Pourfallah, M., Gholinia, M., Armin, M., & Ghadi, A. Z. (2022). Thermofluids analysis of combustion, emissions, and energy in a biodiesel (C11H22O2) / natural gas heavy-duty engine with RCCI mode (Part I: Single/ two -stage injection). *International Journal of Thermofluids*, *16*, 100227. 10.1016/j.ijft.2022.100227

XI. Maliha, A., & Abu-Hijleh, B. (2023). A review on the current status and post-pandemic prospects of third-generation biofuels. *Energy Systems*, *14*(4), 1185–1216. 10.1007/s12667-022-00514-7

XII. Mi, S., Wu, H., Pei, X., Liu, C., Zheng, L., Zhao, W., Qian, Y., & Lu, X. (2023). Potential of ammonia energy fraction and diesel pilot-injection strategy on improving combustion and emission performance in an ammonia-diesel dual fuel engine. *Fuel*, *343*, 127889. 10.1016/j.fuel.2023.127889

XIII. Motallebi Hasankola, S. S., Shafaghat, R., Jahanian, O., & Nikzadfar, K. (2020). An experimental investigation of the injection timing effect on the combustion phasing and emissions in reactivity-controlled compression ignition (RCCI) engine. *Journal of Thermal Analysis and Calorimetry*, *139*(4), 2509–2516. 10.1007/s10973-019-08761-0

XIV. Nazemi, M., & Shahbakhti, M. (2016). Modeling and analysis of fuel injection parameters for combustion and performance of an RCCI engine. *Applied Energy*, *165*, 135–150. 10.1016/j.apenergy.2015.11.093

XV. Soloiu, V., Rivero-Castillo, A., Muinos, M., Duggan, M., Harp, S., Peavy, W., Wolter, S., & Vlcek, B. (2014). *Simultaneous Reduction of NO_X and Soot in a Diesel Engine through RCCI Operation with PFI of n-butanol and DI of Cottonseed Biodiesel*. 2014-01–1322. 10.4271/2014-01-1322

XVI. Thomas, J. J., Nagarajan, G., Sabu, V. R., Manojkumar, C. V., & Sharma, V. (2022). Performance and emissions of hexanol-biodiesel fuelled RCCI engine with double injection strategies. *Energy*, *253*, 124069. 10.1016/j.energy.2022.124069

XVII. Yasin, N. H. M., Aziz, N. N. C., Azmai, M. B. A., & Hanapi, M. F. M. (2023). Transesterification method of microalgae biomass to produce fatty acid methyl esters. *Journal of Chemical Technology & Biotechnology*, *98*(11), 2774–2783. 10.1002/jctb.7338.

XVIII. R. V. Kadupu, K. S. Jafar, and P. V. Elumalai, "Physiochemical Analysis of Hydrogen-Enriched Waste Plastic Oil: Implications for Injection Timing and Combustion Efficiency," *Int. J. Automot. Technol.*, vol. 27, no. 2, pp. 789–802, Apr. 2026. 10.1007/s12239-025-00322-9.

XIX. E. P.V, "Graphene Oxide Nanoparticle Blended Tamanu Methyl Ester as a Promising Alternative Fuel for Unmodified Compression Ignition Engine," *Int. Res. J. Multidiscip. Technovation*, pp. 151–164, Jan. 2025, 10.54392/irjmt25111.